IL NUOVO CIMENTO **46 C** (2023) 19
DOI 10.1393/ncc/i2023-23019-8

Colloquia: La Thuile 2022

A second resonance of the Higgs field: Theoretical motivations and experimental signals

Maurizio Consoli
INFN - Sezione di Catania - I-95129 Catania, Italy

received 19 September 2022

Summary. — Analytical arguments and lattice simulations indicate that, beside the known resonance of mass $m_h = 125\,\mathrm{GeV}$, defined by the quadratic shape of the effective potential at its minimum, the Higgs field could exhibit a second heavier excitation with mass $(M_H)^{\mathrm{theor}} = 690 \pm 10$ (stat) $\pm\, 20$ (sys) GeV. This larger M_H would measure the zero-point energy and, differently from m_h, would remain finite in units of the weak scale $\langle\Phi\rangle \sim 246.2\,\mathrm{GeV}$ for an ultraviolet cutoff $\Lambda_s \to \infty$. In spite of its large mass, however, the heavier state would couple to longitudinal W's with the same typical strength of the low-mass state at 125 GeV. As such, its total decay width Γ_H would be much smaller than the conventional expectation and its main production mechanism at LHC would be through gluon-gluon fusion (ggF). For an experimental check I have thus considered the ATLAS sample of 4-lepton ggF-like events in the region of invariant mass $\mu_{4l} = 620$–$740\,\mathrm{GeV}$ ($l = e, \mu$) which extends about $\pm 60\,\mathrm{GeV}$ around our central mass value. These data indicate the presence of a new resonance with mass $(M_H)^{\mathrm{exp}} = 660$–$680\,\mathrm{GeV}$ and reproduce, to high accuracy, a characteristic correlation, between resonating peak cross section $\sigma_R(pp \to H \to 4l)$ and the ratio $\gamma_H = \Gamma_H/M_H$. This correlation is nearly insensitive to the precise value of Γ_H and mainly determined by the lower mass $m_h = 125\,\mathrm{GeV}$. Therefore, one could also fit m_h from the 4-lepton data in the high-mass range 620–740 GeV. The result $(m_h)^{\mathrm{fit}} \sim (125 \pm 13)\,\mathrm{GeV}$ reproduces the direct measurement of the Higgs particle mass and supports the idea that m_h and the new $(M_H)^{\mathrm{exp}}$ are the masses of two different excitations of the same field.

1. – Introduction

Today, the Higgs field spectrum is described as a single narrow resonance of mass $m_h = 125\,\mathrm{GeV}$ defined by the quadratic shape of the effective potential at its minimum. If Spontaneous Symmetry Breaking (SSB) is a second-order phase transition, this is the PDG view [1] with scalar potential

$$V_{\mathrm{PDG}}(\varphi) = -\frac{1}{2}m^2_{\mathrm{PDG}}\varphi^2 + \frac{1}{4}\lambda_{\mathrm{PDG}}\varphi^4. \tag{1}$$

For $m_{\mathrm{PDG}} \sim 88.8\,\mathrm{GeV}$ and $\lambda_{\mathrm{PDG}} \sim 0.13$, this has a minimum at $|\varphi| = \langle\Phi\rangle \sim 246\,\mathrm{GeV}$ and a second derivative $V''_{\mathrm{PDG}}(\langle\Phi\rangle) \equiv m_h^2 = (125\,\mathrm{GeV})^2$.

However, recent lattice simulations of Φ^4 in 4D [2-4] support instead the view of SSB as a (weak) 1st-order phase transition. While in the presence of gauge bosons SSB is often described as a 1st-order transition, recovering this result in pure Φ^4 requires to replace standard perturbation theory with some alternative scheme. The implications of a 1st-order scenario in pure Φ^4 have not been fully exploited because, with a finite but very large cutoff, besides the 125 GeV resonance, there could be another much larger mass scale M_H associated with the zero-point energy. Since vacuum stability would depend on M_H, and not on m_h, SSB could originate within the pure scalar sector regardless of the other parameters of the theory, *e.g.*, the vector boson and top quark mass.

For more details, I address to refs. [5-7] where, as schemes for a (weak) first-order transition in Φ^4, one explored the original Coleman-Weinberg [8] one-loop calculation and the Gaussian effective potential [9, 10]. Indeed, in both cases, SSB occurs when the quanta of the symmetric phase have a tiny but still positive mass squared. These two calculations, corresponding to different re-summations of graphs, support each other and admit the same physical interpretation: an effective potential $V_{\text{eff}}(\varphi)$ given by some classical background + zero-point energy of a particle with some $\varphi-$dependent mass $M(\varphi)$. As a result, in both approximations, by defining m_h^2 as $V''_{\text{eff}}(\varphi)$ at the minimum and M_H as $M(\varphi)$ at the minimum, in terms of the ultraviolet cutoff Λ_s, one finds

$$L = \ln(\Lambda_s/M_H) \sim \frac{1}{\lambda}, \qquad M_H^2 \sim L m_h^2 \gg m_h^2. \tag{2}$$

With these two mass scales, which do not scale uniformly, the correct renormalization pattern is obtained by requiring the standard non-interacting continuum limit for the fluctuations around the minimum of the potential ("triviality"). Then, with the usual relations $m_h^2 = \lambda\langle\Phi\rangle^2/3$ and $\lambda \sim 16\pi^2/(3L)$, one finds cutoff-independent M_H and $\langle\Phi\rangle$.

To further clarify the $m_h - M_H$ difference, let us recall that the derivatives of the effective potential produce (minus) the n-point functions at zero external momentum. Hence m_h^2, which is $V''_{\text{eff}}(\varphi)$ at the minimum, is directly the 2-point function $|\Pi(p=0)|$. On the other hand, the zero-point energy is (one-half of) the trace of the logarithm of the inverse propagator $G^{-1}(p) = (p^2 - \Pi(p))$. Thus M_H^2 effectively reflects some average value $|\langle\Pi(p)\rangle|$ at larger p^2 so that, if $M_H \neq m_h$, there must be a non-trivial momentum dependence of $\Pi(p)$([1]).

This two-mass structure was checked with lattice simulations of the propagator [5]. By computing m_h^2 from the $p \to 0$ limit of $G(p)$ and M_H^2 from its behaviour at higher p^2, the lattice data indicate two different regimes and a propagator [7] of the form

$$G(p) \sim \frac{1 - I(p)}{2}\frac{1}{p^2 + m_h^2} + \frac{1 + I(p)}{2}\frac{1}{p^2 + M_h^2}, \tag{3}$$

where the interpolating function $I(p)$ depends on an intermediate momentum scale p_0 and tends to $+1$ for large $p^2 \gg p_0^2$ and to -1 when $p^2 \to 0$. Notably, the lattice data were consistent with the increasing logarithmic trend $M_H^2 \sim L m_h^2$ in the continuum limit([2]).

([1]) This explains the different cutoff dependence of m_h and M_H. Indeed, the "triviality" of Φ^4 requires a continuum limit with just a massive free-field propagator. Thus, for $\Lambda_s \to \infty$, there are only two possibilities: either the usual perturbative limit $m_h/M_H = 1 + O(\lambda) \to 1$ or their non-uniform scaling, see [7].

([2]) Equation (3) resembles van der Bij's two-pole propagator [11] indicating that (one-loop)

Since, differently from m_h, the larger M_H remains finite in units of $\langle\Phi\rangle \sim 246.2$ GeV for $\Lambda_s \to \infty$, one can derive their proportionality relation. To this end, let us express M_H^2 in terms of $m_h^2 L$ through some constant c_2, say $M_H^2 = m_h^2 L \cdot (c_2)^{-1}$ and replace the leading-order estimate $\lambda \sim 16\pi^2/(3L)$ in the relation $\lambda = 3m_h^2/\langle\Phi\rangle^2$. Then one finds $M_H = K\langle\Phi\rangle$ with $K \sim (4\pi/3)\cdot(c_2)^{-1/2}$. Since, from a fit to the lattice propagator [5], we found $(c_2)^{-1/2} = 0.67 \pm 0.01$ (stat) $\pm\, 0.02$ (sys) this gives the estimate

$$M_H = 690 \pm 10 \text{ (stat)} \pm 20 \text{ (sys) GeV}. \tag{4}$$

In this theoretical framework, I will describe in sect. **2** the basic phenomenology of the new resonance and then resume in sect. **3** the analysis of [14] of the ATLAS 4-lepton data in the range 620–740 GeV [15]. These data suggest a new resonance consistently with eq. (4) and, even more significantly, reproduce a particular correlation with the lower-resonance mass at 125 GeV. Finally, sect. **4** will contain the conclusions.

2. – The new resonance and its basic phenomenology

For the "triviality" of Φ^4 theories in 4D, the Λ_s-independent combination $3K^2 = 3M_H^2/\langle\Phi\rangle^2$ *cannot* determine observable processes. In this sense, $3K^2$ is basically different from the coupling λ governed by the β-function

$$\ln\frac{\mu}{\Lambda_s} = \int_{\lambda_0}^{\lambda} \frac{\mathrm{d}x}{\beta(x)}. \tag{5}$$

For $\beta(x) = 3x^2/(16\pi^2) + O(x^3)$, whatever the contact coupling λ_0 at the asymptotically large Λ_s, at finite scales $\mu \sim M_H$ this gives $\lambda \sim 16\pi^2/(3L)$ with $L = \ln(\Lambda_s/M_H)$.

Notice [16, 7] that there is no contradiction with the original calculation [17] in the unitary gauge. There, a large M_H in the Higgs propagator was making very high-energy $W_L W_L$ scattering similar to $\chi\chi$ Goldstone boson scattering with contact coupling $\lambda_0 = 3K^2$. However this is a tree approximation with the same coupling at all momentum scale. To describe $W_L W_L$ scattering at some scale μ one should first use the $\beta-$function to re-sum higher-order effects in $\chi\chi$ scattering

$$A(\chi\chi \to \chi\chi)\Big|_{g_{\rm gauge}=0} \sim \lambda \sim \frac{1}{\ln(\Lambda_s/\mu)} \tag{6}$$

and then use the Equivalence Theorem [18-20] which gives

$$A(W_L W_L \to W_L W_L) = [1 + O(g^2_{\rm gauge})]\; A(\chi\chi \to \chi\chi)\Big|_{g_{\rm gauge}=0} = O(\lambda). \tag{7}$$

Thus the large coupling $\lambda_0 = 3K^2$ is actually replaced by the much smaller coupling

$$\lambda = \frac{3m_h^2}{\langle\Phi\rangle^2} = 3K^2\;\frac{m_h^2}{M_H^2} \sim 1/L. \tag{8}$$

---

radiative corrections will feel an effective mass $m_{\rm eff}$ with $m_h \le m_{\rm eff} \le M_H$, see [7]. Thus, one should check how well the mass from radiative corrections agrees with the $m_h = 125$ GeV, measured directly at LHC. Here it is crucial the positive $m_{\rm eff} - \alpha_s(M_z)$ correlation [12], with $\alpha_s(M_z)$ giving the strong-interaction correction to the quark-parton model in $\sigma(e+e^- \to hadrons)$ at energy $Q = M_z$. Since the most complete analysis of $e+e^- \to hadrons$ data [13], for $20\,\text{GeV} \le Q \le 209\,\text{GeV}$, indicates an overall 4-sigma excess with $\alpha_s(M_z) \gtrsim 0.128$, the present view, that the Higgs mass parameter from radiative corrections agrees perfectly with the $m_h = 125$ GeV measured at LHC, is not free of ambiguities.

Analogously, the conventional large width into longitudinal W's computed with $\lambda_0 = 3K^2$, say $\Gamma^{\rm conv}(H \to W_L W_L) \sim M^3_H/\langle\Phi\rangle^2$, should be rescaled by $(\lambda/3K^2) = m^2_h/M^2_H$. This gives

$$\Gamma(H \to W_L W_L) \sim \frac{m^2_h}{M^2_H}\, \Gamma^{\rm conv}(M_H \to W_L W_L) \sim M_H\, \frac{m^2_h}{\langle\Phi\rangle^2}, \tag{9}$$

where M_H indicates the available phase space in the decay and $m^2_h/\langle\Phi\rangle^2$ the interaction strength. For the reference value $M_H = 700\,\text{GeV}$, where $\Gamma^{\rm conv}(H \to ZZ) \sim 56.7\,\text{GeV}$ [22], this gives

$$\Gamma(H \to ZZ) \sim \frac{m^2_h}{(700\ \text{GeV})^2}\ 56.7\ \text{GeV} \tag{10}$$

so that for $m_h = 125\,\text{GeV}$ one finds $\Gamma(H \to ZZ) \sim 1.8\,\text{GeV}$.

Besides, in [21, 7] one was also assuming $\Gamma(H \to \text{fermions} + \text{gluons} + \text{photons}\ldots) \sim 28\,\text{GeV}$ and the ratio $\Gamma(H \to W^+W^-)/\Gamma(H \to ZZ) \sim 2.03$, from [22], deducing a total width $\Gamma(H \to all) \sim 33.5\,\text{GeV}$ and a fraction $B(H \to ZZ) \sim (1.8\ /\ 33.5) \sim 0.054$. However, these estimates were not inluding the new contributions to the total width from the decays of the heavier state into the lower-mass state at 125 GeV. These include the two-body decay $H \to hh$, the three-body decays $H \to hhh$, $H \to hZZ$, $H \to hW^+W^-$ and all higher-multiplicity final states allowed by phase space. Therefore, the above value $\Gamma(H \to all) \sim 33.5\,\text{GeV}$ should only be considered as a lower bound and the fraction $B(H \to ZZ) \sim (1.8\ /\ 33.5) \sim 0.054$ as an upper bound.

Since it is not easy to evaluate these additional contributions, I will now discuss a test that does *not* require the knowledge of the total width. To this end, I will consider the 4-lepton channel and a certain excess of events in the ATLAS data around 680 GeV [15] by only relying on two assumptions:

i) a resonant 4-lepton production through the chain $H \to ZZ \to 4l$;

ii) the value eq. (10) and the linear scaling for small variations around $M_H = 700\,\text{GeV}$

$$\Gamma(H \to ZZ) \sim \frac{M_H}{700\ \text{GeV}} \cdot \frac{m^2_h}{(700\ \text{GeV})^2}\ 56.7\ \text{GeV}. \tag{11}$$

Therefore, by defining $\gamma_H = \Gamma(H \to all)/M_H$, we find a fraction

$$B(H \to ZZ) = \frac{\Gamma(H \to ZZ)}{\Gamma(H \to all)} \sim \frac{1}{\gamma_H} \cdot \frac{56.7}{700} \cdot \frac{m^2_h}{(700\ \text{GeV})^2}, \tag{12}$$

that will be replaced in the cross section approximated by on-shell branching ratios

$$\sigma_R(pp \to H \to 4l) \sim \sigma(pp \to H) \cdot B(H \to ZZ) \cdot 4B^2(Z \to l^+l^-). \tag{13}$$

This should be a good approximation for a relatively narrow resonance, whose virtuality should be small, so that one gets the anticipated correlation

$$\gamma_H \cdot \sigma_R(pp \to H \to 4l) \sim \sigma(pp \to H) \cdot \frac{56.7}{700} \cdot \frac{m^2_h}{(700\ \text{GeV})^2} \cdot 4B^2(Z \to l^+l^-). \tag{14}$$

TABLE I. – *The ATLAS ggF-like 4-lepton events for the four different categories.*

E [GeV]	MVA-high-4μ	MVA-high-2e2μ	MVA-high-4e	MVA-low	ToT
635(15)	2	0	1	7	10
665(15)	0	2	2	17	21
695(15)	1	0	1	9	11
725(15)	0	1	0	3	4

Since $4B^2(Z \to l^+l^-) \sim 0.0045$, the last needed ingredient is the production cross section $\sigma(pp \to H)$. As discussed in [21, 7], the relevant production in our picture is through gluon-gluon Fusion (ggF). In fact, the Vector-Boson Fusion (VBF) plays no role in our model(3). Thus, I will replace $\sigma(pp \to H) \to \sigma^{\rm ggF}(pp \to H)$ in eq. (14) and use the ggF cross sections taken from the updated Handbook of Higgs cross sections [24], see table 1 of [14]. For 13 TeV pp collisions, and taking into account a typical $\pm 15\%$ uncertainty due to the choice of the parton distributions, of the QCD scale..., this gives the estimate $\sigma^{\rm ggF}(pp \to H) \sim 1180(180)$ fb which also accounts for the range $M_H = 660$–700 GeV. Therefore, for $m_h = 125$ GeV, we arrive to the theoretical prediction

$$[\gamma_H \cdot \sigma_R(pp \to H \to 4l)]^{\rm theor} \sim (0.0137 \pm 0.0021)\ {\rm fb}. \tag{15}$$

3. – Analysis of the ATLAS 4-lepton events

To check eq. (15), we have considered [14] the ATLAS sample [15] of 4-lepton data for invariant mass $\mu_{4l} = 620$–740 GeV ($l = e, \mu$) which extends about ± 60 GeV around our central mass value eq. (4). Now, eq. (15) accounts for H-production via the ggF mechanism and ignores VBF production which plays no role in our picture. Therefore, one should compare with that subset of data that, for their characteristics, admit this interpretation. To this end, the ATLAS experiment has performed a Multivariate analysis (MVA) of the ggF production mode which divides the events into four mutually exclusive categories: ggF-MVA-high-4μ, ggF-MVA-high-2e2μ, ggF-MVA-high-4e, ggF-MVA-low. The four sets were extracted from the corresponding HEPData file [25] and are reported in table I.

By transforming the total number of ggF 4-lepton events in table I into cross sections, for the given luminosity 139 fb^{-1}, and defining $s = E^2$, we also assumed the interference of a resonating amplitude $A^R(s) \sim 1/(s - M_R^2)$ with a smooth background $A^B(s)$. For a positive interference below peak, setting $M_R^2 = M_H^2 - iM_H\Gamma_H$, this gives a total cross

(3) The $VV \to H$ process (here $VV = W^+W^-, ZZ$) is the inverse of the $H \to VV$ decay so that $\sigma^{\rm VBF}(pp \to H)$ can be expressed [23] as a convolution with the parton densities of the same Higgs resonance decay width. The traditional importance of this mechanism depends on the conventional large width into longitudinal W's and Z's computed with the $3K^2$ coupling. In our case, where this width is rescaled by the small ratio $(125/700)^2 \sim 0.032$, one finds $\sigma^{\rm VBF}(pp \to H) \lesssim 10$ fb which can be safely neglected.

TABLE II. – *For each γ_H we report the values of M_H, peak cross section σ_R and product $k = \gamma_H \cdot \sigma_R$ obtained from a fit with eq. (16) to the total ATLAS events in table I.*

γ_H	M_H [GeV]	σ_R [fb]	$k = \gamma_H \cdot \sigma_R$ [fb]
0.05	678(6)	0.218(39)	0.0109(20)
0.06	676(7)	0.191(30)	0.0115(18)
0.07	673(10)	0.174(26)	0.0122(18)
0.08	669(20)	0.161(24)	0.0129(19)
0.09	668(16)	0.151(22)	0.0136(20)
0.10	668(15)	0.141(21)	0.0141(21)
0.11	669(15)	0.133(21)	0.0146(23)
0.12	670(16)	0.125(22)	0.0150(26)
0.13	672(17)	0.118(23)	0.0153(30)
0.14	673(19)	0.112(26)	0.0157(36)
0.15	674(20)	0.106(29)	0.0159(43)

section

$$\sigma_T = \sigma_B - \frac{2(s-M_H^2)\ \Gamma_H M_H}{(s-M_H^2)^2 + (\Gamma_H M_H)^2}\ \sqrt{\sigma_B \sigma_R} + \frac{(\Gamma_H M_H)^2}{(s-M_H^2)^2 + (\Gamma_H M_H)^2}\ \sigma_R, \tag{16}$$

where, in principle, both the average background σ_B, at the central energy 680 GeV, and the resonating peak cross-section σ_R can be treated as free parameters.

In a first series of fits to the ATLAS data, for each given $\gamma_H = \Gamma_H/M_H$, there were 3 free parameters, namely M_H, σ_R and σ_B. As a control, we then repeated the analysis by assuming the background to be a decreasing function of energy depending on a parameter fixing the slope of $\sigma_B(E)$ at $E = 680$ GeV. The second series of fits did not show appreciable evidence for an energy-decreasing background so that we reported in table II the results with a constant average background. The profile of the χ^2 as function of γ_H and the fit to the ATLAS cross sections for $\gamma_H = 0.09$ are reported respectively in fig. 1 and in fig. 2.

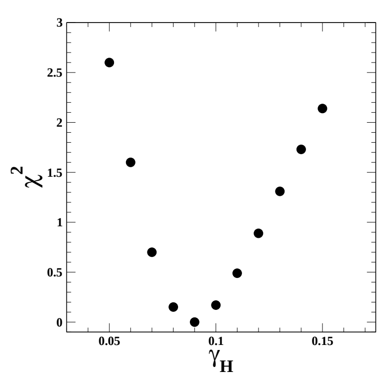

Fig. 1. – At the various γ_H, the chi-square of the fit with eq. (16) to the ATLAS data.

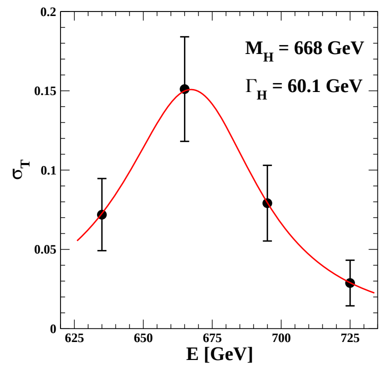

Fig. 2. – For $\gamma_H = 0.08$, we show the fit with eq. (16) to the ATLAS cross sections in fb.

I have also reported in fig. 3 the peak cross sections of table II and compared with the shaded area enclosed by the two hyperbolae $\sigma_R = (0.0137 \pm 0.0021)/\gamma_H$. This picture illustrates how well the observed $\gamma_H - \sigma_R$ correlation in table II is reproduced by our theoretical model eq. (15). In particular, notice the agreement between eq. (15) and the value $k = \gamma_H \cdot \sigma_R = 0.0136(20)$ for $\gamma_H = 0.09$ which gives the minimum χ^2. Finally, a fit to all entries in table II with $\chi^2 < 1$ gives

$$[\gamma_H \cdot \sigma_R(pp \to H \to 4l)]^{\rm fit} = k \sim (0.0137 \pm 0.0008)\ {\rm fb}. \tag{17}$$

Therefore, with our estimate $\sigma(pp \to H) \sim \sigma^{\rm ggF}(pp \to H) \sim 1180(180)$ fb, we find

$$(m_h)^{\rm fit} \sim (125 \pm 13)\ {\rm GeV}, \tag{18}$$

whose central value coincides with the measured Higgs particle mass.

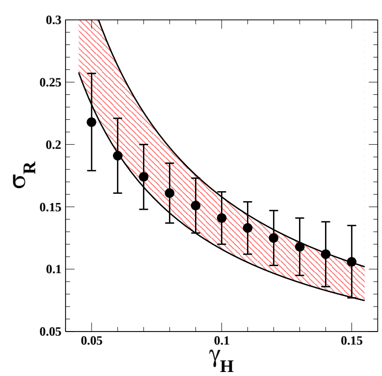

Fig. 3. – The σ_R's of Table 2 are compared with our theoretical prediction eq. (15) represented by the shaded area enclosed by the two hyperbolae $\sigma_R = (0.0137 \pm 0.0021)/\gamma_H$.

4. – Summary and conclusions

From the phenomenological analysis of sect. **3**, we can draw the following conclusions:

i) Table II suggests a new resonance of mass 660–680 GeV consistently with eq. (4).

ii) Our prediction eq. (15) coincides with the corresponding eq. (17) obtained from a fit to the ATLAS 4-lepton data. Equivalently, the central value of the fitted lower-mass state $(m_h)^{\text{fit}} \sim (125 \pm 13)\,\text{GeV}$ coincides with the direct, experimental value $m_h = 125\,\text{GeV}$.

iii) Consistently with our picture, in the ATLAS analysis there is no sizeable contribution from the VBF production mode to the new resonance (on average, only 2 VBF-like events *vs.* 46 ggF-like events, see fig. 2e of ref. [15]).

iv) re-obtaining exactly the same central value $m_h = 125\,\text{GeV}$ means that, for $M_H \sim 680\,\text{GeV}$, a ggF cross section of about 1180 fb and the ATLAS selection criteria of ggF-like events are consistent to a high level of precision

v) the correlation successfully reproduced in fig. 3 effectively eliminates the spin-zero *vs.* spin-2 ambiguity in the interpretation of the heavy state.

Therefore, our picture of a second resonance of the Higgs field finds support in the present ATLAS 4-lepton data. Given the importance of the issue, an analogous comparison with CMS would be important. Unfortunately, this can only be done with smaller statistical samples because in the full $137\,\text{fb}^{-1}$ CMS analysis [26], all data in the range 600–800 GeV were summarized into a single bin of 200 GeV. However, with a, hopefully, forthcoming analysis of data in 20–30 GeV bins, as made by ATLAS, the correlation could be checked again. In this case, the whole issue of the second resonance could be settled now, before the start of RUN3. Of course, for a complete analysis, one should also look at the other final states. For this reason, I will close this paper by mentioning the (local) 3-sigma excess, see fig. 3 of [27], observed in the ATLAS $\gamma\gamma$ distribution for the same invariant-mass $\mu_{\gamma\gamma} \sim 680\,\text{GeV}$ obtained from our analysis of the 4-lepton data. Even though the global statistical significance is reduced to less than 2-sigma, by the looking-elsewhere effect, still this particular excess of events represents the highest peak in fig. 3 of [27].

* * *

I thank Leonardo Cosmai for his precious collaboration. I also thank Giorgio Bellettini, Giorgio Chiarelli, Mario Greco and Gino Isidori for their invitation to the Conference.

REFERENCES

[1] Particle Data Group (Tanabashi M. *et al.*), *Phys. Rev. D*, **98** (2018) 030001.
[2] Lundow P. H., Markström K., *Phys. Rev. E*, **80** (2009) 031104.
[3] Lundow P. H., Markström K., *Nucl. Phys. B*, **845** (2011) 120.
[4] Akiyama S. *et al.*, *Phys. Rev. D*, **100** (2019) 054510.
[5] Consoli M., Cosmai L., *Int. J. Mod. Phys. A*, **35** (2020) 2050103, hep-ph/2006.15378.
[6] Consoli M., Cosmai L., *Symmetry*, **12** (2020) 2037.
[7] Consoli M., *Acta Phys. Pol. B*, **52** (2021) 763, arXiv:2106.06543 [hep-ph].

[8] Coleman S. R., Weinberg E. J., *Phys. Rev. D*, **7** (1973) 1888.
[9] Barnes T., Ghandour G. I., *Phys. Rev. D*, **22** (1980) 924.
[10] Stevenson P. M., *Phys. Rev. D*, **32** (1985) 1389.
[11] van der Bij J. J., *Acta Phys. Pol. B*, **11** (2018) 397.
[12] Consoli M., Hioki Z., *Mod. Phys. Lett. A*, **10** (1995) 845.
[13] Schmitt M., arXiv:hep-ex/0401034v2.
[14] Consoli M., Cosmai L., arXiv:2111.08962v2 [hep-ph].
[15] ATLAS Collaboration (Aad G. *et al.*), *Eur. Phys. J. C*, **81** (2021) 332, arXiv:2009.14791[hep-ex].
[16] Castorina P., Consoli M., Zappalà D., *J. Phys. G*, **35** (2008) 075010, arXiv:hep-ph/0710.0458.
[17] Lee B. W., Quigg C., Tacker H. B., *Phys. Rev. D*, **16** (1977) 1519.
[18] Cornwall J. M., Levin D. N., Tiktopoulos G., *Phys. Rev. D*, **10** (1974) 1145.
[19] Chanowitz M. S., Gaillard M. K., *Nucl. Phys. B*, **261** (1985) 379.
[20] Bagger J., Schmidt C., *Phys. Rev. D*, **41** (1990) 264.
[21] Consoli M., Cosmai L., arXiv:2007.10837v2 [hep-ph].
[22] LHC Higgs Cross Section Working Group (Dittmaier S. *et al.*), arXiv:1101.0593 [hep-ph].
[23] Kane G. L., Repko W. W., Rolnick W. B., *Phys. Lett. B*, **148** (1984) 367.
[24] `https://twiki.cern.ch/twiki/bin/view/LHCPhysics/CERNYellowReportPageAt1314TeV2014`.
[25] `https://www.hepdata.net/record/ins1820316`.
[26] CMS Collaboration (Sirunyan A. M. *et al.*), *Eur. Phys. J. C*, **81** (2021) 200.
[27] ATLAS Collaboration (Aad G. *et al.*), *Phys. Lett. B*, **822** (2021) 136651.